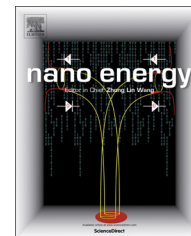


Available online at [www.sciencedirect.com](http://www.sciencedirect.com)

ScienceDirect

journal homepage: [www.elsevier.com/locate/nanoenergy](http://www.elsevier.com/locate/nanoenergy)

## OPINION

# The effect of SrTiO<sub>3</sub>:ZnO as cathodic buffer layer for inverted polymer solar cells



Jo-Lin Lan<sup>a</sup>, Zhiqiang Liang<sup>a</sup>, Yi-Hsun Yang<sup>a</sup>, Fumio S. Ohuchi<sup>a</sup>,  
Samson A. Jenekhe<sup>b</sup>, Guozhong Cao<sup>a,\*</sup>

<sup>a</sup>Department of Material Science and Engineering, University of Washington, Seattle, WA 98195, USA

<sup>b</sup>Department of Chemical Engineering, University of Washington, Seattle, WA 98195, USA

Received 18 September 2013; accepted 21 December 2013

Available online 4 January 2014

## KEYWORDS

Inverted polymer solar cells;  
Cathodic buffer layer;  
SrTiO<sub>3</sub>:ZnO;  
P3HT:PCBM;  
Bulk heterojunction

## Abstract

Dual phase SrTiO<sub>3</sub>:ZnO nanocomposite films with varied composition ratios were fabricated by sol-gel processing and applied as cathodic buffer layers (CBL) for inverted polymer solar cells, and demonstrated enhanced power conversion efficiency. Basic properties of SrTiO<sub>3</sub>:ZnO CBL films were examined by means of XRD, XPS, AFM, UV-vis absorption spectra, and goniometry. When the cathodic buffer layers were assembled to solar cells, the device properties including incident photon-to-current conversion efficiency (IPCE), power conversion efficiency, and electron mobility were investigated systematically. SrTiO<sub>3</sub> in CBL was found to be amorphous or quasicrystalline. Although more detailed experiments are needed, SrTiO<sub>3</sub> is more likely to have some local ordering structure with aligned TiO<sub>6</sub> octahedra, i.e., quasicrystalline phase, and thus possesses spontaneous polarization as reported in the literature (Frenkel et al., 2005 [1]; Frenkel et al., 2007 [2]; Ehre et al., 2007 [3]; Ehre et al., 2007 [4]; Ehre et al., 2007 [5]). Such spontaneous polarization is likely to induce a self-built electric field to prevent electron recombination on the interface of the bulk heterojunction (BHJ) active layer and cathodic buffer layer (CBL), and result in high power conversion efficiency.

© 2014 Published by Elsevier Ltd.

## Introduction

Polymer solar cells (PSCs) have undoubtedly caught world-wide attention due to its acceptable energy conversion efficiency, potential to furnish low cost solar electricity, and capability to achieve portable application [6–10]. Based on electron flow

directions in the devices, PSCs can be divided into two main structures: the conventional and inverted structures.

A conventional structure of PSCs consists of the bulk heterojunction (BHJ) active layer made by blending polymer donor [11–13] with fullerene acceptor [14,15] in organic solvents and spin-coated on the top of indium tin oxide (ITO) glass modified by the hole transporting layer (HTL), such as, poly(3,4 ethylenedioxyethynaphthalene):poly(styrene sulfonic acid) (PEDOT:PSS), molybdenum oxide (MoO<sub>x</sub>), etc. [16–19]. A low work function metal served as the top electrode,

\*Corresponding author. Tel.: +1 206 616 9084.

E-mail address: [gzcao@u.washington.edu](mailto:gzcao@u.washington.edu) (G. Cao).

typically aluminum, is evaporated on the top of BHJ layer. Excitons generated in the BHJ active layer then separate to electrons and holes, and electrons will be transported and collected on the top electrode; holes, on the other hand, will diffuse and go through the ITO glass to the external load. The conventional structure can be represented as: ITO/hole transporting layer (HTL)/(BHJ) active layer/Al. Enormous progress has been made recently through design and synthesis of new low band gap donor polymers, control of nano and microstructures of active polymer layers, and optimization of solar cell device structures, leading to a great advancement in power conversion efficiency, 10.2%, the highest record achieved to date [20], very close to dye-sensitization solar cells with 12.3% [21], and amorphous silicon solar cells with 13.4% [22]. Despite the rapid development of new low band gap donor polymers, and the significant advancement in power conversion efficiency, conventional structure polymer solar cells suffer from rapid performance degradation due to low work function top electrode, and unstable interface between ITO substrate and HTL [29-34], which is unacceptable for practical applications.

In the inverted PSC structure, on the contrary, the electron flow path is opposite to that of the conventional one. A cathodic buffer layer, usually metal oxide, such as ZnO, TiO<sub>x</sub>, Nb<sub>2</sub>O<sub>5</sub>, Cs<sub>2</sub>CO<sub>3</sub>, or Al<sub>2</sub>O<sub>3</sub> [19, 23-33], is deposited on ITO glass to reduce its work function in order to lower the barrier of electron transfer to the ITO electrode. In addition, this kind of metal oxide needs to have the hole blocking and electron collecting ability to enhance the power conversion efficiency [34]. The top electrode is replaced by high work function metal, such as silver, to fulfill hole collection. The entire inverted structure changes to ITO/metal oxide layer/(BHJ) active layer/hole transporting layer (HTL)/Ag. Recently, the study on inverted PSCs is very common since inverted structure can improve the stability of conventional structure by replacing the air sensitive, low work function top electrode (aluminum) with a stable, high work function one (silver or gold), and also eliminate the interface between the acidic PEDOT:PSS hole transporting layer and ITO glass. With an appropriately fabricated cathodic buffer layer, the inverted polymer solar cells have demonstrated much improved cyclic stability [35,36]. However, compared with conventional PSCs, inverted structure PSCs typically possess a relatively low power conversion efficiency possibly due to the electron loss on the interface between the BHJ active layer and the metal oxide layer. For example, the best conventional P3HT:PCBM device exhibited 4.4% PEC, slightly higher than the best inverted device (4.2%) from the same lab [37]. It is possible for inverted polymer solar cells to achieve comparable power conversion efficiency with the conventional structure polymer solar cells if the charge loss at the interface of cathodic buffer layer is reduced [37]. Hence, numerous studies focus on the surface modification of metal oxide with self-assembled monolayers, such as C<sub>60</sub>-SAMs, saline or C<sub>60</sub> molecules [38-42], manipulating its morphology and surface energy, and new material doping to enhance its electron collecting ability, such as Al-doped ZnO (AZO), Ga-doped ZnO (GZO), and zinc tin oxide (ZTO) [43-45].

In this paper, we introduced a quasi-amorphous perovskite complex metal oxide strontium titanate (SrTiO<sub>3</sub>) admixed with zinc oxide (ZnO) by sol-gel processing as

cathodic buffer layers for inverted structure PSCs. Perovskite complex metal oxides, ABO<sub>3</sub>, do not have a close packed anion lattice and thus offer a number of possibilities in manipulation of its chemical composition and crystal structure to achieve various desired physical and chemical properties. Most of them are ferro-, pyro- and piezoelectrics as the cations inside the oxygen octohedra have a large space to rattle, leading to high dielectric constant [46]. The high dielectric constants (300-20,000) are the combination of both large atomic/electronic polarization in large-sized cations, and large ionic polarization as a result of large rattling space for cations inside oxygen octohedra [47,48]. Compared with ZnO, SrTiO<sub>3</sub> has a higher dielectric constant ( $\sim 10^4$ ) [49], similar band gap structure [50], but lower electron mobility [51]. Such a high dielectric constant material would favor the effective charge transfer in PSCs [52]. In addition, the cations inside the oxygen octohedra are commonly small in radius, making the six coordinated structure stable only at high temperatures. At low temperatures, the cations would shift away from the center of the deformed oxygen octohedra and result in a separation of positive and negative charge centers, or better known as spontaneous polarization [1-5]. It was hypothesized that the material with larger dielectric constant and spontaneous polarization, such as SrTiO<sub>3</sub>, may create an internal electric field while PSCs operation [53]. By tuning the SrTiO<sub>3</sub>:ZnO ratio in the cathodic buffer layers, the power conversion efficiency of the inverted PSCs was found to vary accordingly. The possible mechanism and influences of the composition, crystallinity, and surface properties of dual phase SrTiO<sub>3</sub>:ZnO nanocomposite CBLs on the photo-to-electrical energy conversion have been discussed.

## Experiment

### Materials

Regioregular poly(3-hexylthiophene-2,5-diyl)(P3HT, 4002-E grade) was purchased from Rieke Metals, Inc. [6,6]-phenyl-C61-butyric acid methyl ester (PCBM, 99.0% purity) was purchased from American Dye Source, Inc. Poly(3,4 ethylenedioxyethiophene):poly(styrene sulfonic acid) (PEDOT:PSS, Clevis 4083) was purchased from H.C. Starck. Zinc acetate (Zn(CH<sub>3</sub>COO)<sub>2</sub>, 98.0%), 2-methoxyethanol (CH<sub>3</sub>OCH<sub>2</sub>-CH<sub>2</sub>OH, 99.0%), amonoethanolamine (NH<sub>2</sub>CH<sub>2</sub>CH<sub>2</sub>OH-2H<sub>2</sub>O, 99.0%), Strontium acetate (Sr(CH<sub>3</sub>COO)<sub>2</sub>, 97.0%), and titanium (IV) isopropoxide (Ti(C<sub>12</sub>H<sub>28</sub>O<sub>4</sub>), 97%) were purchased from Sigma-Aldrich. All the chemicals were used as received without further purification.

ITO glass (10-15 Ω/sq) substrates were purchased from Colorado Concept Coatings LLC. Samples were prepared on ITO substrates (1.5 × 1.5 cm<sup>2</sup>), which were cleaned prior to use by ultrasonic agitation in a detergent solution, acetone, and isopropyl alcohol, and then dried under nitrogen flow.

### Preparation of the SrTiO<sub>3</sub>:ZnO cathodic buffer layers

#### ZnO sol preparation

Zinc acetate hydrate was first dissolved in a mixture of 2-methoxy ethanol and monoethanolamine at room temperature.

The concentration of zinc acetate is 0.1 M and the molar ratio of monoethanolamine to zinc acetate was 1:1. The resulting solution was stirred using a magnetic stirrer at 60 °C for 2 h to yield a homogeneous, clear, and transparent sol.

#### SrTi(OR)<sub>x</sub> sol preparation

Strontium acetate was added in acetic acid and stirred till it was completely dissolved. Acetylacetone was added as a stabilizing agent, then titanium (IV) isopropoxide slowly added to the solution by drip. The final concentration of SrTi(OR)<sub>x</sub> sol is 0.1 M and it was kept stirring at room temperature for 2 h to form a homogeneous, yellow, and transparent sol.

#### SrTi(OR)<sub>x</sub>:ZnO sol preparation

Both SrTi(OR)<sub>x</sub> and ZnO sol's concentration are 0.1 M, and simply mixed these two sols with a molar ratio (SrTi(OR)<sub>x</sub>:ZnO=0:100, 5:95, 10:90, 15:85, 20:80, 25:75) to form SrTiO<sub>3</sub>:ZnO sol.

The SrTiO<sub>3</sub>:ZnO layers were spin-coated after the prepared solution was aged at room temperature for one day in order to make it more glutinous. The sols were dropped onto ITO glass substrates, which were then spun at 3000 rpm for 30 s. After processing, the samples were immediately baked at 300 °C for 10 min and subsequently annealed at 350 °C for 20 min in air to convert metal oxide. Throughout the device fabrication process, we fixed all the process parameters except for SrTiO<sub>3</sub>:ZnO sol composition.

#### Device fabrication and characterization

The chlorobenzene solution of P3HT:PCBM (1:0.8 by weight) containing (20 mg/mL) P3HT and (16 mg/mL) PCBM was stirred in glovebox at 60 °C overnight. The solution was allowed to cool to room temperature and then filtered through a 0.2 μm polytetrafluoroethylene (PTFE) filter. First, the P3HT:PCBM blend solution was spin-coated onto the ITO substrates with the SrTiO<sub>3</sub>:ZnO buffer layer at 700 rpm for 30 s. Then the samples were baked at 225 °C for 1 min to help in self-organization of P3HT, as well as to drive away residual solvent and assist in the polymer contact with the SrTiO<sub>3</sub>:ZnO cathodic buffer layer. Then, the diluted PEDOT:PSS (Clevios PVP AL 4083) solution was spin-coated onto the active layer to form the hole-transport

layer. The films were then baked at 120 °C for 10 min. A 100 nm thick Ag film was finally deposited under a vacuum of  $2 \times 10^{-6}$  Torr as the top electrode. The device structure of space-charge-limited-current (SCLC) measurement is the same, only without the PEDOT:PSS layer.

The *I*-*V* characteristics of the solar cell were tested in a glovebox using a Keithley 2400 source measurement unit and an Oriel Xenon lamp (450 W) coupled with an AM1.5 filter. A silicon solar cell certificated by the national renewable energy laboratory (NREL) was used as a reference to calibrate the measurement conditions. The light intensity used in this study was 100 mW/cm<sup>2</sup>.

#### SrTiO<sub>3</sub>:ZnO buffer layer characterization

The surface morphologies of the specimens were obtained using AFM (Asylum Research MFP-3D Stand Alone AFM) operated in the tapping mode. Optical transmittance spectra were recorded using a Thermo Fisher Scientific (EVO30 PC) UV-vis recording spectrophotometer over the wavelength range between 300 and 900 nm. XPS spectra and secondary electron cutoff were generated using a PHI Versaprobe system with an Al K $\alpha$  X-ray source and a 100 μm beam size. The work function value was calibrated with a pure gold foil (5.1 eV). Measurements were taken while the sample was under ultrahigh vacuum ( $10^{-10}$  Torr). The contact angle was measured by a goniometer, and each sample was measured four times in different areas. X-ray diffraction patterns were measured by Bruker F8 Focus Powder XRD. The X-ray source is Cu-K-alpha radiation and the scale range between 20° and 80°.

#### Results and discussion

Figure 1 represents the inverted PSCs structure and the corresponding energy level diagram in this study. The only difference in all devices in this study was the amount of SrTiO<sub>3</sub> in cathodic buffer layer (CBL), while all the other components, such as thickness of P3HT/PCBM, annealing process, and measurement parameters, were kept the same. The amount of SrTiO<sub>3</sub> in ZnO sol was controlled from 0% to 25% (molar ratio), and in order to understand the basic properties of this new material, UV-vis absorption spectra, contact angle, atomic force microscopy (AFM), X-ray diffraction (XRD), and X-ray photoelectron spectroscopy (XPS)

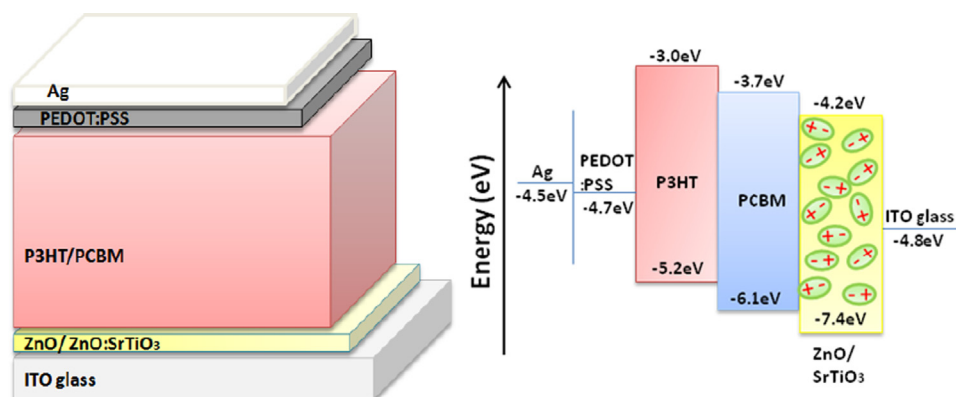
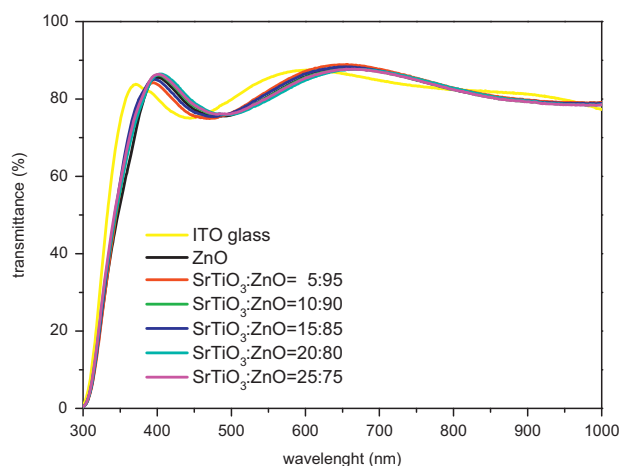


Figure 1 Inverted structure of PSCs and the corresponding energy level diagram of the components of the devices.



**Figure 2** The UV-vis spectra of ITO glass and various SrTiO<sub>3</sub>:ZnO/ITO glass.

were applied to examine the surface morphology, properties and chemical composition. The cathodic buffer layer's transmittance in the visible light region is important in inverted structure since the incident light has to pass through the film first and be absorbed by the BHJ active layer [54]. Figure 2 is the UV-vis absorption spectra of various SrTiO<sub>3</sub>:ZnO thin films, and it is found that the UV-vis absorption spectra have no significant difference regardless of the amount of SrTiO<sub>3</sub>, and all SrTiO<sub>3</sub>:ZnO films have good optical transmittance in the visible region and, thus, is suitable to serve as a cathodic buffer layer in inverted polymer solar cells.

Figure 3 shows the AFM and contact angle images of SrTiO<sub>3</sub>:ZnO CBL, and the root mean square (RMS) surface roughness and contact angle value are summarized in Table 1. The thickness of CBL is about 10 nm as measured by AFM, and does not change with the amount of SrTiO<sub>3</sub> added into the film, the surface roughness of various SrTiO<sub>3</sub>:ZnO films is around 2.4 nm, and the morphology is similar to each other. The contact angle of the films with various SrTiO<sub>3</sub>:ZnO ratio is in the range of 37–39°, which means that the surface energy has little change with the addition of SrTiO<sub>3</sub>, and all the films are slightly hydrophilic.

The X-ray diffraction patterns of SrTiO<sub>3</sub>:ZnO=20:80 with various thermal annealing conditions are illustrated in Figure 4 (a), and it can be observed that there are only ZnO characteristic peaks under the 350 and 500 °C annealing processes, and SrTiO<sub>3</sub> and Zn<sub>2</sub>TiO<sub>4</sub> characteristic peaks appeared when the annealing temperature was increased to 900 °C. Owing to the thermal restriction of ITO glass substrate, 350 °C - 20 min was applied to anneal the SrTiO<sub>3</sub>:ZnO films used as cathodic buffer layers in inverted polymer solar cells studied in the present investigation. So in such cathodic buffer layers, no detectable crystalline SrTiO<sub>3</sub> was formed. Figure 4(b) compares the XRD patterns of SrTiO<sub>3</sub>:ZnO=20:80 and pure ZnO annealed at 350 °C; the intensity of ZnO characteristic peaks is not proportional to the amount of ZnO in CBL. Such a low diffraction peak intensity and signal to noise ratio are strong indications of low crystallinity and/or low content of crystalline phase of ZnO in the SrTiO<sub>3</sub>:ZnO composite films. The relatively low crystallinity of ZnO in SrTiO<sub>3</sub>:ZnO films is reasonable; the presence of SrTiO<sub>3</sub>

in CBL is likely to interfere and retard the ZnO crystallization during thermal annealing [55]. Furthermore, SrTiO<sub>3</sub>:ZnO=20:80 film has Zn<sub>2</sub>TiO<sub>4</sub> characteristic peaks after 900 °C annealing, which suggests that some portion of ZnO in the film remained in the amorphous phase under low temperature annealing process.

Surface chemical analysis was carried out by means of X-ray photoelectron spectroscopy (XPS) (Figure 5) and the work function was calculated using the secondary electron cut-off region; the surface element distribution and work function are summarized in Table 2. As shown in Figure 5, the intensities of Zn 2p (1021.8 eV) and 3S (139.8 eV) peaks decrease with the increasing amount of SrTiO<sub>3</sub>. On the other hand, the intensities of Ti 2p (458.8 eV) and Sr 3d (134.3 eV) peaks increase with the increasing SrTiO<sub>3</sub> amount in CBL. The binding energy of Ti 2p<sub>3/2</sub> is located at 458.8 eV which shows that SrTiO<sub>3</sub> was formed on the surface [56].

The approximate composition of the SrTiO<sub>3</sub>:ZnO surface can be determined by dividing the individual peak areas by their respective atomic sensitivity factor (ASF). Since there is no database of metal oxide's ASF, we simply used the calculated ASF with SrTiO<sub>3</sub>:ZnO=15:85 as the standard to obtain various SrTiO<sub>3</sub>:ZnO films' surface composition. From Figure 5(b) and Table 2, it was found that the amount of strontium is similar to the SrTiO<sub>3</sub>:ZnO sol precursor solution, and the work function of SrTiO<sub>3</sub>:ZnO decreases with the increasing amount of SrTiO<sub>3</sub> from -4.2 eV for pure ZnO film to -4.53 eV (SrTiO<sub>3</sub>:ZnO with a molar ratio of 25:75); the low work function is favorable to electron transfer from the BHJ active layer to the cathodic buffer layer in the inverted polymer solar cell application [57].

SrTiO<sub>3</sub>:ZnO films with various amounts of SrTiO<sub>3</sub> are applied as cathodic buffer layers in inverted polymer solar cells, and the power conversion efficiencies are summarized in Table 3, and *I*-*V* curves are shown in Figure 6. From Table 3, compared with pure ZnO CBL, with a small amount of SrTiO<sub>3</sub> (<15%) addition, the fill factor is found to increase from 0.57 to 0.65, and the open circuit voltage also increases slightly from 0.61 to 0.63 V, whereas the short circuit current remains almost constant at around 10 mA/cm<sup>2</sup>. As a result, the overall power conversion efficiency increases from 3.58% to 4.1%. However, if the amount of SrTiO<sub>3</sub> is greater than 15%, the power conversion efficiency starts to reduce, and it is caused by the decrease in fill factor, which is probably attributable to the smaller electron mobility in SrTiO<sub>3</sub>, as will be discussed further later in the paper. The maximum power conversion efficiency was achieved in an inverted PSC with the cathodic buffer layer consisting of SrTiO<sub>3</sub> 10%.

The IPCE spectra are shown in Figure 7; since the short circuit current of each device is similar, there is no significant difference in IPCE spectra with various SrTiO<sub>3</sub> amounts. This observation is very reasonable considering the fact that the optical transmittance through the buffer layers remains the same regardless of the amount of SrTiO<sub>3</sub> and thus the amount of photons entering the polymer layers is the same. The open circuit voltage increase from 0.61 to 0.63 V with the addition of SrTiO<sub>3</sub> might be due to SrTiO<sub>3</sub>:ZnO's work function decreasing from -4.2 to -4.5 eV while SrTiO<sub>3</sub> was added. The cathodic buffer layer's work function decrease is favorable to electron transfer from the BHJ active layer to the cathodic buffer layer and result in higher *V*<sub>oc</sub> [57].

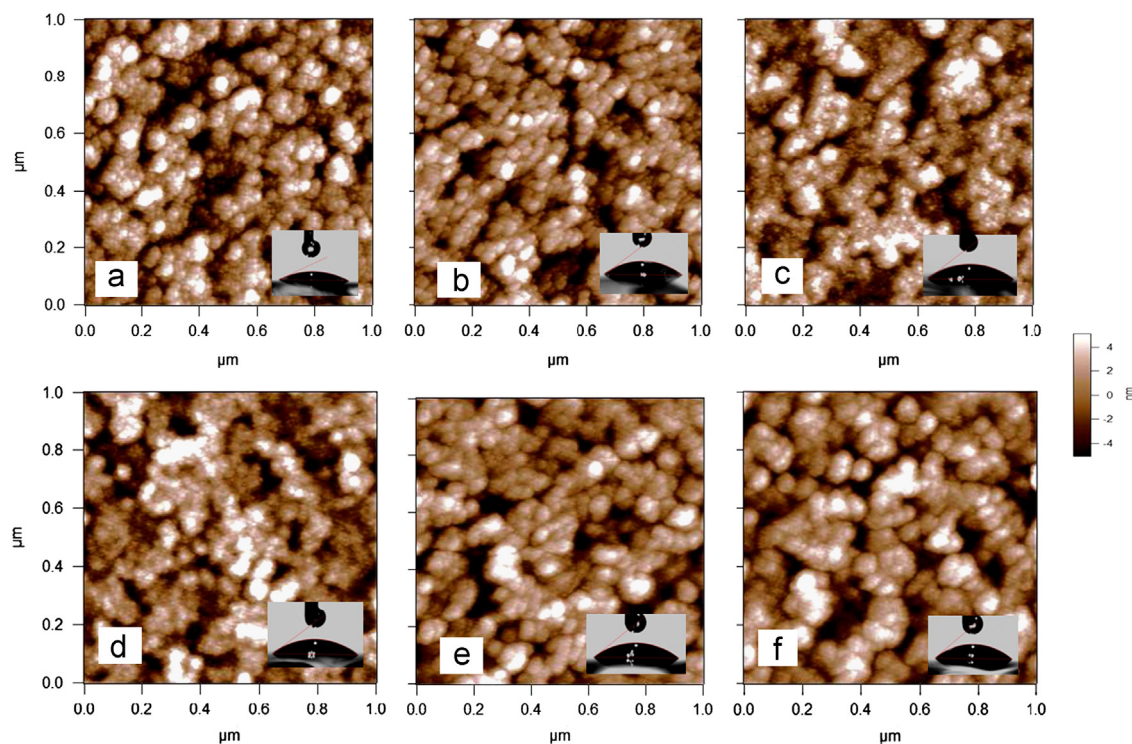


Figure 3 The surface morphology and contact angle of various SrTiO<sub>3</sub>:ZnO/ITO glasses.

Table 1 The root mean square (RMS) surface roughness and contact angle of various SrTiO<sub>3</sub>:ZnO/ITO glasses.

Device	Roughness (nm)	Contact angle (deg)
Pure ZnO	2.49	38.1
SrTiO <sub>3</sub> :ZnO=5:95	2.38	37.5
SrTiO <sub>3</sub> : ZnO=10:90	2.45	38.3
SrTiO <sub>3</sub> : ZnO=15:85	2.30	37.6
SrTiO <sub>3</sub> : ZnO=20:80	2.41	39
SrTiO <sub>3</sub> : ZnO=25:75	2.48	39.8

Fill factor can be contributed by series and shunt resistance in the device, and it can be calculated by the inverse of the slope near  $V_{oc}$  and  $J_{sc}$  to represent the overall resistance and the recombination in the device, respectively. Compared with the pure ZnO buffer layer, the cathodic buffer layer with a small amount of SrTiO<sub>3</sub> (<15%) has the same series resistance but larger shunt resistance, which means that electron recombination can be reduced by the addition of SrTiO<sub>3</sub>, leading to a larger fill factor. While increasing the amount of SrTiO<sub>3</sub> to 20% or 25%, the large series resistance becomes predominant, and results in low power conversion efficiency.

SrTiO<sub>3</sub>:ZnO films could possess some local ordering structure with aligned TiO<sub>6</sub> octohedra; small-scale TiO<sub>6</sub>

octohedra local ordering might have spontaneous polarization as it is in crystalline perovskite [1-5]. In this study, the CBL went through a thermal annealing process, with an anisotropic heating to induce the anisotropic stress/strain in SrTiO<sub>3</sub>:ZnO films. In turn, the presence of anisotropic stress/strain might induce some local ordering of TiO<sub>6</sub> octohedra. The crystalline ITO glass substrate directly in contact with SrTiO<sub>3</sub>:ZnO films may also induce some local ordering. Such spontaneous polarization is likely to induce a self-built electric field while polymer solar cells are functioning. As shown in Figure 8, the localized polar molecules SrTiO<sub>3</sub> in the cathodic buffer layer are in random orientations in the dark condition or open circuit voltage condition when there is no net electron flow in the device (Figure 8(a)). However, while incident light is absorbed by the BHJ active layer and generates excitons to form electrons and holes pair, the electrons and holes go through different directions and form a net electron field, which will polarize SrTiO<sub>3</sub>:ZnO films by orienting the dipole moments of local ordering polar molecules (Figure 8(b)). A similar concept is applied by the self-assembled monolayer (SAM) treatment on the ZnO surface with different dipole orientations and a substituent on the 4-position of benzoic acid [53].

With a small amount of local ordering SrTiO<sub>3</sub> in the cathodic buffer layer, the positive interface dipole might retard hole transport through the cathodic buffer layer, and reduce the electron recombination on the interface of the BHJ active layer and the cathodic buffer layer, which shows fill factor improves the device performance. However, while the SrTiO<sub>3</sub> amount is too much, the positive interface dipole becomes too strong to let any electron pass through. Therefore, device performance encumbers with large electron transfer resistance on the interface of the BHJ active

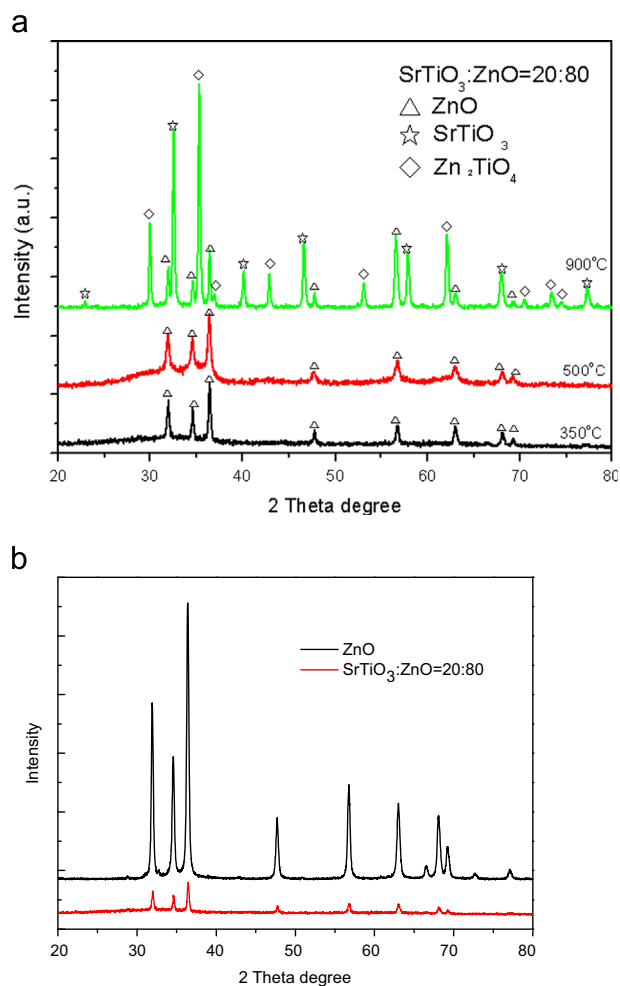


**Figure 4** (a) XRD patterns of SrTiO<sub>3</sub>:ZnO=20:80 under various temperature annealing processes. (b) XRD patterns of pure ZnO and SrTiO<sub>3</sub>:ZnO=20:80. Annealing temperature: 350 °C.

layer and the cathodic buffer layer, resulting in low fill factor and poor performance.

In order to directly measure the resistance of the cathodic buffer layer (CBL), we fabricate the device's structure (ITO/CBL/Al) and measure its linear sweep voltammetry (Figure 9). Since the thickness of CBL is only 10 nm, the whole device is ohm contact. The inverse of the slope ( $I/V$ ) can represent the resistance of CBL. The results show that the CBL's resistance has a similar trend as the series resistance obtained from the  $I-V$  curve, which also directly indicates that the reason for increase in series resistance in the device is due to the SrTiO<sub>3</sub> amount.

The electron mobility of the SrTiO<sub>3</sub>:ZnO film is determined by fitting the dark  $J-V$  curves for single carrier devices with the SCLC model [58]. The electron-only devices structure was ITO/SrTiO<sub>3</sub>:ZnO/P3HT:PCBM/Al fabricated to evaluate the electron mobility of the SrTiO<sub>3</sub>:ZnO film by the charge transfer model of SCLC. The current is given by  $J = 9/8 \times \epsilon_0 \times \epsilon_r \times \mu_e \times V^2/D^3$ , where  $\epsilon_0$  is the permittivity of free space,  $\epsilon_r$  is the relative permittivity of PCBM,  $\mu_e$  is the electron mobility, and  $D$  is the thickness of the active layer.

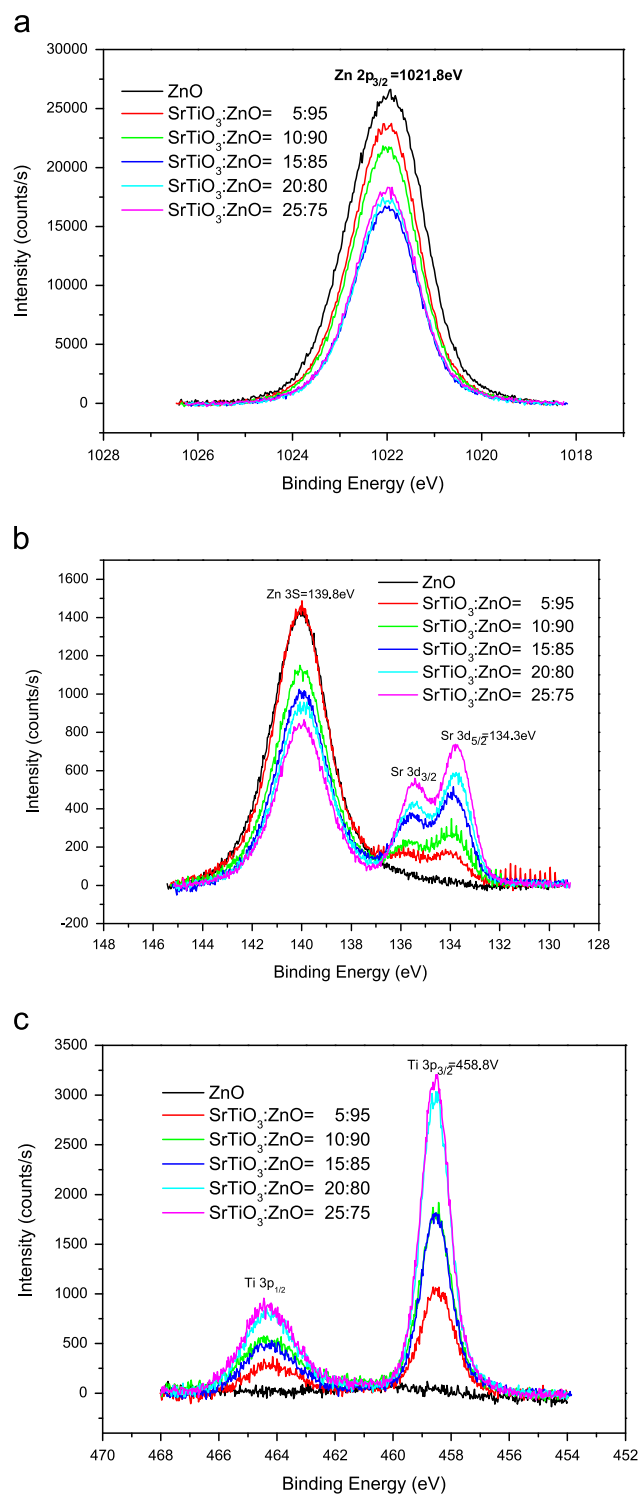


**Figure 5** XPS results of various SrTiO<sub>3</sub>:ZnO films. Core levels of (a) Zn 2p. (b) Zn 3S and Sr 3d. (c) Ti 3p.

From Table 3, compared with pure ZnO ( $3.76 \times 10^{-7} \text{ m}^2 \text{ V}^{-1} \text{ s}^{-1}$ ), the electron mobility of 5% and 10% SrTiO<sub>3</sub>:ZnO remain in the same level as pure ZnO ( $\sim 10^{-7} \text{ m}^2 \text{ V}^{-1} \text{ s}^{-1}$ ). With continued increase of the SrTiO<sub>3</sub> amount, the electron mobility begins to drop ( $\sim 10^{-9} \text{ m}^2 \text{ V}^{-1} \text{ s}^{-1}$ ), which can correlate with the poor power conversion efficiency results.

**Table 2** The element amount fitting results and the value of work function of various SrTiO<sub>3</sub>:ZnO/ITO glasses. The XPS scan range: 130–145 eV. The value of work function was calculated by secondary electron cutoff region. The atomic sensitivity factor (ASF) of Zn and Sr is ASF<sub>Zn</sub>=0.03567 and ASF<sub>Sr</sub>=0.007684, respectively.

Device	Sr 3d area	Zn 3S area	SrTiO <sub>3</sub> (%)	ZnO (%)	Work function (eV)
Pure ZnO	0	3627	0	100	−4.2
SrTiO <sub>3</sub> :ZnO=5:95	201	3502	2.41	97.59	−4.39
SrTiO <sub>3</sub> :ZnO=10:90	503	2630	7.61	92.39	−4.43
SrTiO <sub>3</sub> :ZnO=15:85	976	2383	14.99	85.01	−4.34
SrTiO <sub>3</sub> :ZnO=20:80	1254	2235	19.47	80.53	−4.36
SrTiO <sub>3</sub> :ZnO=25:75	1656	1935	26.94	73.06	−4.53

**Table 3** *I*-*V* characteristics of inverted PSCs with various SrTiO<sub>3</sub>:ZnO films as the cathodic buffer layer.

Device	V <sub>oc</sub> (V)	J <sub>sc</sub> (mA/cm <sup>2</sup> )	FF	Efficiency (%)	R <sub>s</sub> (Ω cm <sup>2</sup> )	R <sub>sh</sub> (kΩ cm <sup>2</sup> )	Electron mobility (m <sup>2</sup> V <sup>−1</sup> s <sup>−1</sup> )
Pure ZnO	0.61	10.16	0.570	3.58	1	6.8	3.76E−07
SrTiO <sub>3</sub> :ZnO=5:95	0.63	9.98	0.627	3.98	0.86	7.9	2.66E−07
SrTiO <sub>3</sub> :ZnO=10:90	0.63	10.08	0.647	4.10	0.88	18.2	1.77E−07
SrTiO <sub>3</sub> :ZnO=15:85	0.63	10.08	0.625	3.99	0.91	20.4	4.43E−08
SrTiO <sub>3</sub> :ZnO=20:80	0.63	9.75	0.484	2.96	3	10.2	1.33E−08
SrTiO <sub>3</sub> :ZnO=25:75	0.63	9.66	0.390	2.38	8.7	6.3	3.32E−09

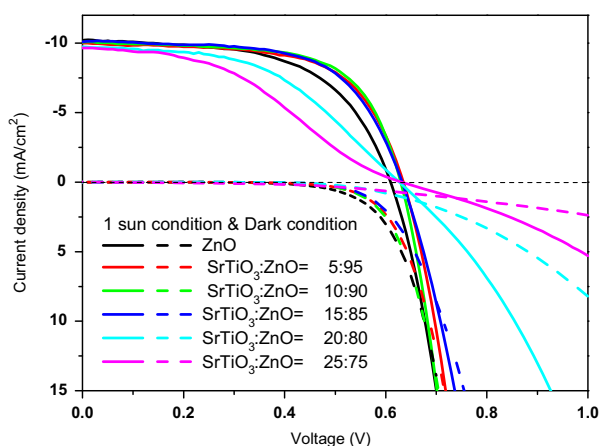


**Figure 6** The *I*-*V* curve at 1 sun and dark condition with various SrTiO<sub>3</sub>:ZnO films as the cathodic buffer layer.

Furthermore, electron transfer through the CBL might also be affected by the crystallinity of CBL. As Figure 4 (b) shows, the intensity of the ZnO peak is enormously reduced in the presence of SrTiO<sub>3</sub>. The low crystallinity of ZnO will affect the electron transfer through CBL, and result in low electron mobility, high series resistance and small fill factor. Further improvement of SrTiO<sub>3</sub>:ZnO CBL can be expected by replacing the amorphous SrTiO<sub>3</sub> with crystal phase as well as improving the crystallinity of ZnO.

It is clear that the admixing SrTiO<sub>3</sub> with ZnO results in a promising cathodic buffer layer for inverted polymer solar cells. However, its full potential has not been explored as the amorphous nature of SrTiO<sub>3</sub> and low crystallinity of ZnO in the sol-gel-derived nanocomposite CBL is seriously

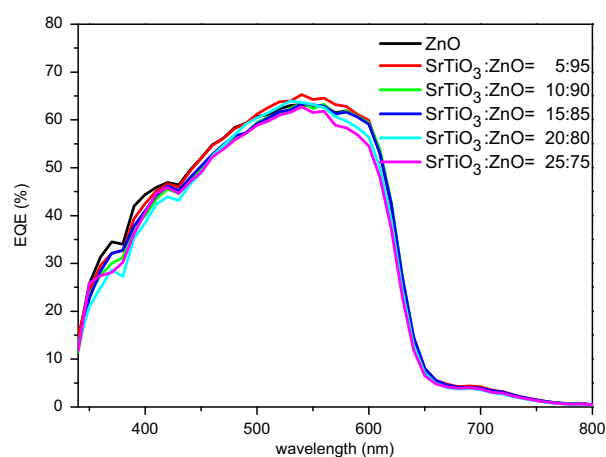


**Figure 7** IPCE results of various SrTiO<sub>3</sub>:ZnO films as cathodic buffer layers.

compromised with low charge transfer property. Although only a modest enhancement in power conversion efficiency from 3.58% to 4.1% was achieved with SrTiO<sub>3</sub>:ZnO of 90:10 CBL, much greater improvement is anticipated if the films are well crystallized for both SrTiO<sub>3</sub> and ZnO.

## Conclusions

Dual phase SrTiO<sub>3</sub>:ZnO nanocomposite films have been fabricated and demonstrated as the cathodic buffer layer in inverted polymer solar cells for an improved power conversion efficiency. The device performance was found to be strongly dependent on the amount of SrTiO<sub>3</sub> in CBL.

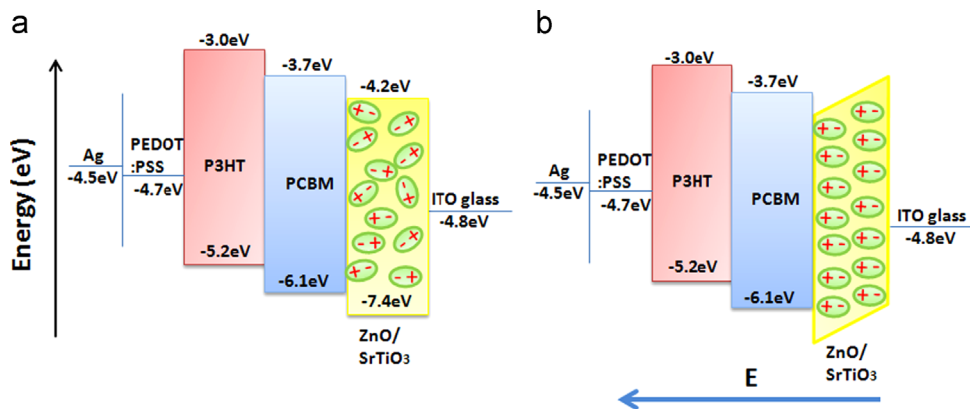


**Figure 8** Schematic energy level diagram of inverted polymer solar cells with SrTiO<sub>3</sub>:ZnO as the cathodic buffer layer. (a) The device is under open circuit condition, and there is no net interface dipole. (b) The device is under illumination, electron field was generated by electron and hole transfer to the opposite direction and there is a net interface dipole directed away from the cathodic buffer layer.

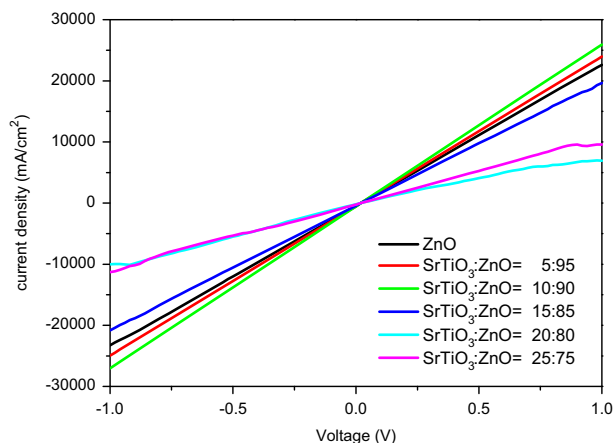


**Figure 9** The linear sweep voltammetry of (ITO/CBL/Al) device, and various SrTiO<sub>3</sub>:ZnO films were served as the cathodic buffer layer.

With a small amount of quasiamorphous SrTiO<sub>3</sub> added in the ZnO film, some local ordering structure with aligned TiO<sub>6</sub> octohedra would likely form spontaneous polarization, and induce a self-built electric field on the interface between the HBJ active layer and CBL, which would prevent hole transport through CBL and reduce electron recombination, resulting in enhanced power conversion efficiency. However, a continued increase in the amount of quasiamorphous SrTiO<sub>3</sub> in the ZnO film led to lower electron mobility. In the present study, it was found that the composition of SrTiO<sub>3</sub>:ZnO at 10:90 offered the best solar cell performance, and the power conversion efficiency increases from 3.58% (pure ZnO) to 4.1%, presenting 15% enhancement.

## Acknowledgment

This work is supported in part by the U.S. Department of Energy, Office of Basic Energy Sciences, Division of Materials Sciences, under Award no. DE-FG02-07ER46467

## References

- [1] A.I. Frenkel, Y. Feldman, V. Lyahovitskaya, E. Wachtel, I. Lubomirsky, *Phys. Rev. B* 71 (2005) 024116.
- [2] A.I. Frenkel, D. Ehre, V. Lyahovitskaya, L. Kanner, E. Wachtel, Igor Lubomirsky, *Phys. Rev. Lett.* 99 (2007) 215502.
- [3] D. Ehre, V. Lyahovitskaya, A. Tagantsev, I. Lubomirsky, *Adv. Mater.* 19 (2007) 1515-1517.
- [4] D. Ehre, H. Cohen, V. Lyahovitskaya, A. Tagantsev, I. Lubomirsky, *Adv. Funct. Mater.* 17 (2007) 1204-1208.
- [5] D. Ehre, H. Cohen, V. Lyahovitskaya, I. Lubomirsky, *Phys. Rev. B* 77 (2008) 184106.
- [6] G. Yu, J. Gao, J.C. Hummelen, F. Wudl, A.J. Heeger, *Science* 270 (1995) 1789-1791.
- [7] W.L. Ma, C.Y. Yang, X. Gong, K. Lee, A.J. Heeger, *Adv. Funct. Mater.* 15 (2005) 1617-1622.
- [8] H.Y. Chen, J. Hou, S. Zhang, Y. Liang, G. Yang, Y. Yang, L. Yu, Y. Wu, G. Li, *Nat. Photonics* 3 (2009) 649-653.
- [9] T. Ameri, G. Dennler, C. Lungenschmied, C.J. Brabec, *Energy Environ. Sci.* 2 (2009) 347-363.
- [10] R. Po, C. Carbonera, A. Bernardi, N. Camaioni, *Energy Environ. Sci.* 4 (2011) 285-310.
- [11] P. Schilinsky, C. Waldauf, C.J. Brabec, *Appl. Phys. Lett.* 81 (2002) 3885.
- [12] J. Peet, J.Y. Kim, N.E. Coates, W.L. Ma, D. Moses, A.J. Heeger, G.C. Bazan, *Nat. Mater.* 6 (2007) 497-500.
- [13] D. Mühlbacher, M. Scharber, M. Morana, Z. Zhu, D. Waller, R. Gaudiana, C. Brabec, *Adv. Mater.* 18 (2006) 2884-2889.
- [14] G. Li, V. Shrotriya, J. Huang, Y. Yao, T. Moriarty, K. Emery, Y. Yang, *Nat. Mater.* 4 (2005) 864-868.
- [15] Y. Liang, Z. Xu, J.B. Xia, S.T. Tsai, Y. Wu, G. Li, C. Ray, L.P. Yu, *Adv. Mater.* 22 (2010) E135-E138.
- [16] G. Heywang, F. Jonas, *Adv. Mater.* 4 (1992) 116-118.
- [17] F. Zhang, M. Johansson, M.R. Andersson, J.C. Hummelen, O. Inganäs, *Adv. Mater.* 14 (2002) 662-665.
- [18] T. Yang, M. Wang, Y. Cao, F. Huang, L. Huang, J. Peng, X. Gong, S.Z.D. Cheng, Y. Cao, *Adv. Energy Mater.* 2 (2012) 523-527.
- [19] Y.J. Cheng, F.Y. Cao, W.C. Lin, C.H. Chen, C.H. Hsieh, *Chem. Mater.* 23 (2011) 1512-1518.
- [20] J. You, C.-C. Chen, Z. Hong, K. Yoshimura, K. Ohya, R. Xu, S. Ye, J. Gao, G. Li, Y. Yang, *Adv. Mater.* 25 (2013) 3973-3978.

- [21] A. Yella, H.-W. Lee, H.N. Tsao, C. Yi, A.K. Chandiran, M. K. Nazeeruddin, W.G. Diau, C.Y. Yeh, S.M. Zakeeruddin, M. Grätzel, *Science* 334 (2011) 629-634.
- [22] S. Kim, J.-W. Chung, H. Lee, J. Park, Y. Heo, H.-M. Lee, *Sol. Energy Mater. Sol. Cells* (2013). <http://dx.doi.org/10.1016/j.solmat.2013.04.016>.
- [23] G. Li, C.W. Chu, V. Shrotriya, J. Huang, Y. Yang, *Appl. Phys. Lett.* 88 (2006) 253503.
- [24] Y. Zhou, H. Cheun, J.W.J. Potscavage, C. Fuentes-Hernandez, S.-J. Kim, B. Kippelen, *J. Mater. Chem.* 20 (2010) 6189-6194.
- [25] Z. Liang, Q. Zhang, O. Wiranwetchayan, J. Xi, Z. Yang, K. Park, C. Li, G. Cao, *Adv. Funct. Mater.* 22 (2012) 2194-2201.
- [26] J.H. Lee, S. Cho, A. Roy, H.-T. Jung, A.J. Heeger, *Appl. Phys. Lett.* 96 (2010) 163303.
- [27] J.P. Liu, K.L. Choy, X.H. Hou, *J. Mater. Chem.* 21 (2011) 1966-1969.
- [28] B. Kumar, S.-W. Kim, *Nano Energy* 1 (2012) 342-355.
- [29] L. Li, T. Zhai, Y. Bando, D. Golberg, *Nano Energy* 1 (2012) 91-106.
- [30] X. Wen, W. Wu, Z.L. Wang, *Nano Energy* (2014).
- [31] A. Hayakawa, O. Yoshikawa, T. Fujieda, K. Uehara, S. Yoshikawa, *Appl. Phys. Lett.* 90 (2007) 163517.
- [32] J.S. Kim, R.H. Friend, F. Cacialli, *Appl. Phys. Lett.* 74 (1999) 3084.
- [33] M.P. de Jong, L.J. van I. doom, A.M.J. de Voigt, *Appl. Phys. Lett.* 77 (2000) 2255.
- [34] K. Kawano, R. Pacios, D. Poplavskyy, J. Nelson, D.D. C. Bradley, J.R. Durrant, *Sol. Energy Mater. Sol. Cells* 90 (2006) 3520-3530.
- [35] S.K. Hau, H.-L. Yip, N.S. Baek, J. Zou, K. O'Malley, A.K.-Y. Jen, *Appl. Phys. Lett.* 92 (2008) 253301.
- [36] M.J. Tan, S. Zhong, J. Li, Z. Chen, W. Chen, *ACS Appl. Mater. Interfaces* 5 (2013) 4696-4701.
- [37] L.M. Chen, Z. Hong, G. Li, Y. Yang, *Adv. Mater.* 21 (2009) 1434-1449.
- [38] X. Bulliard, S.G. Ihn, S. Yun, Y. Kim, D. Choi, J.Y. Choi, M. Kim, M. Sim, J.H. Park, W. Choi, K. Cho, *Adv. Funct. Mater.* 20 (2010) 4381-4387.
- [39] S.K. Hau, Y.J. Cheng, H.L. Yip, Y. Zhang, H. Ma, A.K.Y. Jen, *ACS Appl. Mater. Interfaces* 2 (2010) 1892-1902.
- [40] T. Shirakawa, T. Umeda, Y. Hashimoto, A. Fujii, K. Yoshino, *J. Phys. D. Appl. Phys.* 37 (2004) 847-850.
- [41] C.T. Chen, F.C. Hsu, S.W. Kuan, Y.F. Chen, *Sol. Energy Mater. Sol. Cells* 95 (2011) 740-744.
- [42] R. Thitima, C. Patcharee, S. Takashi, Y. Susumu, *Solid-State Electron.* 53 (2009) 176-180.
- [43] S. Park, S.J. Tark, J.S. Lee, H. Lim, D. Kim, *Sol. Energy Mater. Sol. Cells* 93 (2009) 1020-1024.
- [44] A.K.K. Kyaw, X. Sun, D.W. Zhao, S.T. Tan, Y. Divayana, H.V. Demir, *IEEE J. Sel. Top. Quantum Electron.* 16 (2010) 1700-1706.
- [45] T.Z. Oo, R.D. Chandra, N. Yantara, R.R. Prabhakar, L.H. Wong, *Org. Electron.* 13 (2012) 870-874.
- [46] C.C. Homes, T. Vogt, S.M. Shapiro, S. Wakimoto, A.P. Ramirez, *Science* 293 (2001) 673-676.
- [47] I. Coondoo, *Ferroelectrics*, InTech Publisher, Rijeka, Croatia, 2010.
- [48] B.D. Fahlman, *Materials Chemistry*, 2nd Edition, Chapter 2: Solid-State Chemistry, Springer 13-156.
- [49] K.A. Muller, H. Burkard, *Phys. Rev. B* 19 (1979) 3593-3602.
- [50] D. Jing, L. Guo, L. Zhao, X. Zhang, H. Liu, M. Li, S. Shen, G. Liu, X. Hu, *Int. J. Hydrog. Energy* 35 (2010) 7087-7097.
- [51] H.I. Yoo, C.R. Song, D.K. Lee, *J. Eur. Ceram. Soc.* 24 (2004) 1259-1263.
- [52] K.M. Noone, S. Subramanian, Q. Zhang, G. Cao, S.A. Jenekhe, D.S. Ginger, *J. Phys. Chem. C* 115 (2011) 24403-24410.
- [53] Y.E. Ha, M.Y. Jo, J. Park, Y.-C. Kang, S.I. Yoo, J.H. Kim, *J. Phys. Chem. C* 117 (2013) 2646-2652.
- [54] A.K.K. Kyaw, X.W. Sun, C.Y. Jiang, G.Q. Lo, D.W. Zhao, D. L. Kwong, *Appl. Phys. Lett.* 93 (2008) 221107.
- [55] O.N. Senkov, D.B. Miracle, *Mater. Res. Bull.* 36 (2001) 2183-2198.
- [56] C.D. Wagner, W.M. Rigg, L.E. Davis, et al., *Handbook of X-ray Photoelectron Spectroscopy*, 3rd edition, Perkin-Elmer Corporation, Eden Prairie, MN, USA, 1979.
- [57] H.H. Liao, L.M. Chen, Z. Xu, G. Li, Y. Yang, *Appl. Phys. Lett.* 92 (2008) 173303.
- [58] V.D. Mihailetschi, J.K.J. van Duren, P.W.M. Blom, J.C. Hummelen, R.A.J. Janssen, J.M. Kroon, M.T. Rispens, W. J.H. Verhees, M.M. Wienk, *Adv. Funct. Mater.* 13 (2003) 43-46.



**Dr. Jo-Lin Lan** is a post-doctoral researcher of Department of Materials Science and Engineering at University of Washington, Seattle, WA. She received her Ph.D. degree (2008-2012), M.S. (2005-2007), and BS (2001-2005) from National Tsing-Hua University in Department of Chemical Engineering, Hsinchu, Taiwan. She also worked on nano-structured catalyst and scale-up process for dye-sensitized solar cells in Tripod Technology Corporation, Hsinchu Lab (2007-2011). She is currently researching nanostructured materials for hybrid polymer solar cells. Dr. Lan can be reached at [jljan@uw.edu](mailto:jljan@uw.edu).



**Zhiqiang Liang** is pursuing Ph.D. in the School of Material Science and Engineering, Harbin Institute of Technology and worked as a visiting student in Department of Materials Science, University of Washington. His current research is focused on the inverted polymer solar cells. Zhiqiang Liang can be reached at [yydzlq@yahoo.com.cn](mailto:yydzlq@yahoo.com.cn).



**Yi-Hsun Yang** is a Ph.D student in Materials Science and Engineering at the University of Washington, Seattle, WA. He received his B. S. and M.S. in Chemistry from National Taiwan University, Taipei, Taiwan. He started his Ph.D. program in 2013 in the University of Washington, Seattle. His research interest is to utilize both chemical synthesis and surface analysis. He can be reached at [yyh1982@uw.edu](mailto:yyh1982@uw.edu).



**Dr. Fumio S. Ohuchi** is a professor of Materials Science and Engineering at the University of Washington. He received his B. S. and M.S. in physics from Sophia University, Tokyo, Japan in 1972 and 1974, respectively, followed by Ph.D. in Materials Science and Engineering from the University of Florida. He then worked as a staff scientist from 1981 to 1991 in the R&D Department at the DuPont Experimental Station. He worked there as a staff scientist, where he developed various "in-situ" techniques to look at metal-ceramics and metal-polymer interfaces. In 1992, he moved to UW, where understanding physical and chemical processes at the material's surfaces and dissimilar interfaces is an overall theme of his research. Dr. Ohuchi can be reached at [ohuchi@uw.edu](mailto:ohuchi@uw.edu).



**Dr. Samson A. Jenekhe** is Boeing-Martin Professor of Engineering, Professor of Chemistry Department of Chemical Engineering at the University of Washington, Seattle, WA. He received his Ph.D. degree from University of Minnesota, MA from University of Minnesota, MS from University of Minnesota, and BS from Michigan Technological University. His current research is focused mainly on organic electronics and

optoelectronics, including thin film transistors, solar cells, and LEDs, Self-assembly and nanotechnology, including block copolymers, nanowires, and multicomponent self-assembly, and polymer science, including synthesis, processing, properties, and photonic applications. Dr. Jenekhe can be reached at [jenekhe@chem.washington.edu](mailto:jenekhe@chem.washington.edu).



**Dr. Guozhong Cao** is Boeing-Steiner Professor of Materials Science and Engineering, Professor of Chemical Engineering, and Adjunct Professor of Mechanical Engineering at the University of Washington, Seattle, WA. He received his Ph.D. degree from Eindhoven University of Technology (the Netherlands), M.S. from Shanghai Institute of Ceramics of Chinese Academy of Sciences, and BS from East China University of Science and Tech-

nology (China). He has published over 260 SCI journal papers, authored and edited 7 books, and presented over 200 invited talks and seminars. His current research is focused mainly on chemical processing of nanomaterials for energy related applications including solar cells, lithium-ion batteries, and supercapacitors. Dr. Cao can be reached at [gzcao@uw.edu](mailto:gzca@uw.edu) or 206-616-9084.